Loss of Citron Kinase Affects a Subset of Progenitor Cells That Alters Late but Not Early Neurogenesis in the Developing Rat Retina

Devi Krishna Priya Karunakaran, Nisarg Chhaya, Christopher Lemoine, Sean Congdon, Amye Black, and Rahul Kanadia

Department of Physiology and Neurobiology, University of Connecticut, Storrs, Connecticut, United States

Correspondence: Rahul Kanadia, Department of Physiology and Neurobiology, 75 North Eagleville Road, U-3156, University of Connecticut, Storrs, CT 06269, USA; rahul.kanadia@uconn.edu.

Submitted: July 18, 2014
Accepted: December 18, 2014

Citation: Karunakaran DKP, Chhaya N, Lemoine C, Congdon S, Black A, Kanadia R. Loss of citron kinase affects a subset of progenitor cells that alters late but not early neurogenesis in the developing rat retina. *Invest Ophthalmol Vis Sci*. 2015;56:787–798. DOI:10.1167/iovs.14-15272

Purpose. To understand how loss of citron kinase (*CitK*) affects retinal progenitor cells (RPCs) in the developing rat retina.

Methods. We compared knockout (KO) and wild-type (WT) retinae by immunohistochemistry. The TdT-mediated dUTP terminal nick-end labeling (TUNEL) assay was performed to determine cell death. Pulse-chase experiments using 5-ethynyl-2'-deoxyuridine (EdU) were carried out to interrogate RPC behavior and in turn neurogenesis.

Results. Reverse transcription–polymerase chain reaction analysis showed that *CitK* was expressed at embryonic day (E)12 and was turned off at approximately postnatal day (P)4. Immunohistochemistry showed CitK being localized as puncta at the apical end of the outer neuroblastic layer (ONBL). Analyses during embryonic development showed that the KO retina was of comparable size to that of WT until E13. However, by E14, there was a reduction in the number of S-phase RPCs with a concomitant increase in TUNEL+ cells in the KO retina. Moreover, early neurogenesis, as reflected by retinal ganglion cell production, was not affected. Postnatal analysis of the retina showed that ONBL in the KO retina was reduced to half the size of that in WT and showed further degeneration. Immunohistochemistry revealed absence of Islet1+ bipolar cells at P2, which was further confirmed by EdU pulse-chase experiments. The CitK KO retinae underwent complete degeneration by P14.

Conclusions. Our study showed that *CitK* is not required for a subset of RPCs before E14, but is necessary for RPC survival post E14. This in turn results in normal early embryonic neurogenesis, but severely compromised later embryonic and postnatal neurogenesis.

Keywords: CitK, retina, progenitor cells, bipolar cells

During retinal development, the balance between self-renewal of retinal progenitor cells (RPCs) versus neurogenesis allows for simultaneous RPC amplification and neurogenesis.[1,2] This produces a functional adult retina with six neuronal subtypes including rod photoreceptors, cone photoreceptors, bipolar cells, horizontal cells, amacrine cells, and retinal ganglion cells, and one glial cell type, Müller glia.[3,4] Early RPCs are multipotent cells that are known to shift in their competence to produce different neurons over time.[5–7] Recently, it has been shown that some RPCs have temporal bias in producing a subset of neurons.[8] Together, this suggests a dynamic regulation of RPC cell division that interprets intrinsic and extrinsic cues to regulate neurogenesis. Cell division in the retina occurs such that the S-phase of the cell cycle occurs at the basal end of the outer neuroblastic layer (ONBL), followed by the interkinetic movement of the nucleus toward the apical end where the M-phase of the cell cycle occurs.[9,10] Furthermore, the plane of cell division at the apical end has been reported to regulate whether an RPC undergoes symmetric versus asymmetric cell division.[11] This process is what regulates RPC amplification versus neurogenesis. It is here that the regulators of cytokinesis can influence symmetric versus asymmetric cell division and in turn regulate retinal development. One such gene that regulates cytokinesis is citron kinase (*CitK*).

CitK is a RhoA effector kinase and is a member of the serine/threonine kinase family.[12,13] The dynamic localization of *CitK* has been implicated in multiple functions during cell division. *CitK* has been shown to move from the cytoplasm to spindle mid-zone, and then is transported in telophase to the cytokinesis furrow.[14] It has been shown in vitro that in the late stages of cytokinesis, *CitK* localizes at the cleavage furrow and regulates the assembly and formation of the contractile ring by di-phosphorylating the myosin regulatory light chain.[15,16] In addition, loss of function studies in Hela cells, using small interfering RNAs, have shown that *CitK* loss results in binucleated cells.[17–21] Importantly, G-C deletion in exon 1 of rat *CitK* gene results in a premature stop codon, resulting in nonsense-mediated decay of the aberrant mRNA.[22] Here, loss of *CitK* results in binucleated progenitor cells in the brain followed by cell death of these progenitor cells, resulting in microcephaly.[23] Interestingly, not all neurogenic cytokineses require *CitK*, as ~50% of all neurons in the *citK* mutant have single normally sized nuclei, while others have binucleated nuclei.[24] The profound effect of loss of *CitK* on brain development suggests similar phenotype in the developing retina, where its expression has been shown to be restricted to

RPCs.[25] Here we present our findings regarding retinal development in *CitK* knockout (KO) rats.

Materials and Methods

Animal Procedures

All procedures with rats were performed in accordance with the animal protocol approved by Institutional Animal Care and Use Committee at the University of Connecticut and in compliance with the ARVO Statement for the Use of Animals in Ophthalmic and Vision Research. Wistar rats from Charles River Laboratory (Wilmington, MA, USA) were used for reverse transcription–polymerase chain reaction (RT-PCR) analysis. All *CitK* mutants (Citk$^{fh/fh}$, flathead rats), heterozygous, and wild-type littermates were generated from a breeding colony maintained at the University of Connecticut.

Reverse Transcriptase-Polymerase Chain Reaction

Retinae from different developmental time points in Wistar rats (embryonic day [E]12, E14, E16, E18, postnatal day [P]0, P4, P10, and P14) were harvested and total RNA prepared in Trizol following the manufacturer's protocol (Invitrogen, Grand Island, NY, USA). For cDNA synthesis, 1 μg total RNA from retinae harvested at various time points was used.[26] Polymerase chain reaction to examine the expression of citron kinase gene was performed with the primers across the gene mentioned in the Table. The RT-PCR thermocycler conditions were for 33 cycles (95°C for 30 seconds; 58°C for 30 seconds; 72°C for 50 seconds). Gapdh was used as control. Primers used to amplify Gapdh are mentioned in the Table. The RT-PCR thermocycler conditions were for 30 cycles (95°C for 30 seconds; 58°C for 30 seconds; 72°C for 50 seconds). All PCR products were resolved on a 2.5% agarose gel. The products were then excised and cloned into pGEMT vector (catalog No. A1360; Promega, Madison, WI, USA) and sequenced with T7 primer to confirm their identities.

5-ethynyl-2'deoxyuridine (EdU) Pulse Experiments

Pregnant heterozygous females at E12 were first weighed and injected with 1 mL 25 mM EdU in PBS per 100-mg body weight and embryos were either harvested 1 hour after at E12 or at E13, E14, or E16. The P0 pups were first weighed and injected with 0.4 mL 25 mM EdU in PBS per 100-mg body weight and retinae were harvested at P4.

Immunohistochemistry (IHC)

All of the experiments were performed on 10–16 μm cryosections obtained from different time points in *CitK* KO, heterozygous, and wild-type (WT) littermates. For embryonic analysis, cryosections were subjected to antigen retrieval as described by the manufacturer (catalog No. H-3300; Vector Laboratories, Burlingame, CA, USA) followed by IHC. The sections were then hydrated in phosphate-buffered saline (PBS, pH 7.4) and washed three times (5 minutes each at room temperature [RT]), followed by incubation with PBTS buffer (blocking/permeabilization buffer) (1× PBS with 0.1% Triton X-100, 0.2% BSA, and 0.02% SDS) for 1 hour at RT. Primary antibody ([product No. 40.2D6, mouse anti-Islet1, 1:300; Developmental Studies Hybridoma Bank, Iowa, IA, USA]; [product No. 556003, mouse anti-Ki67; BD Biosciences, San Jose, CA, USA]; [product No. IHC-00061, rabbit anti–Phospho Histone H3 (PH3), 1:300; Bethyl Laboratories, Inc., Montgomery, TX, USA]; [product No. PRB-278P, rabbit anti-Pax6, 1:300; Covance, Dedham, MA, USA]; [product No. MABN15, mouse anti-rhodopsin, clone 4D2, 1:300; Millipore, Billerica, MA, USA]; and [product No. AB5405, rabbit anti-red/green opsin, 1:300; Millipore]) was incubated in PBTS buffer overnight at 4°C. Sections were washed with PBTS buffer containing 4′, 6-diamidino-2-phenylindole (DAPI; Roche Diagnostics, Indianapolis, IN, USA) 10 times (15 minutes each at RT). Following the washes, secondary antibody ([product No. 21206, anti-rabbit antibody conjugated with Alexa488, 1:750; Invitrogen] and [product No. A10037, anti-mouse conjugated with Alexa 568, 1:750; Invitrogen]) was incubated in PBTS buffer overnight at 4°C. Sections were washed with PBTS buffer seven times (15 minutes each at RT), rinsed with PBS, and mounted in Prolong Gold Antifade reagent (Invitrogen) and coverslip glass.

For the detection with mouse anti-CRIK/CitK antibody (product No. 611376, 1:50; BD Biosciences), IHC protocol as described above was used except that the blocking buffer consisted of 1× PBS with 0.5% Triton X-100, 5% normal goat serum (NGS) containing DAPI, followed by the incubation of the primary antibody in permeabilization buffer (1× PBS with 0.25% Triton X-100 and 2.5% NGS) overnight at 4°C. Sections were washed three times with the permeabilization buffer, followed by the incubation with secondary antibody in permeabilization buffer for 2 hours at RT. Sections were washed with permeabilization buffer five times (10 minutes each at RT), rinsed with PBS, and covered with Prolong Gold Antifade reagent and coverslip glass.

For EdU detection, Click-iT EdU Alexa Fluor 647 Imaging Kit (catalog No. C10340; Molecular Probes, Grand Island, NY, USA) was used. The steps were followed as per instructions in the user manual.

TUNEL Assay

In Situ Cell Death Detection Kit, TMR red (catalog No. 12156792910; Roche Diagnostics) and TUNEL Apo-Green Detection Kit (catalog No. B31112; Biotool, Houston, TX, USA) were used to assay the cell death in the embryonic retinal tissue at E14 and E16 as per instructions in the user manual. For determining whether the dying cells were retinal progenitor cells, first, IHC with mouse anti-Ki67 was per-

Table. List of Primers Used in the RT-PCR Analysis

Primer Name (No. Represents Exon)	Primer Sequence (5′–3′)
F1	CGGTAGCGGAGAGATGTTGAAGTTCAAGT
R3	TAACCACCTGCACTTCGGCGAAGT
F3	ACTTCGCCGAAGTGCAGGTGGTTA
R8	GCAACAGAGACCCTCGAACTTCAGTCTCT
F8	AGAGACTGAAGTTCGAGGGTCTCTGTTGC
F8/9	AATAACATCCGGAACTCTCCTCCCC
R12	GCTCTCTGATGTCGTGGAGAAGCTGAAGA
F12	TCTTCAGCTTCTCCACGACATCAGAGAGC
RC13	AGGTCCTTAGCACTCGCTAAGCCA
R14	CTGGAACATTCTCCCACTTCAGGCT
R17	TCCTTCAGTCTGTTCTCTCTACGCTCCATG
F16	TGCAGAACATCCGGCAGGCAAA
R30	AGGGCGAGCTTCAGCTCATTGTACTG
F29	CACGAGAAGGTGAAAATGGAAGGCA
R41	CCGATGAGGATACTGTAATTGGTGAAGTGG
F35	GGTGGAAGAATTTGAGCTGTGCCTTC
R46	TCTGTCCGGCCCTCTCTGTCTCGGTA
GAPDH Fwd	ACAGTCAAGGCCGAGAATGGGAA
GAPDH Rev	TCAGATGCCTGCTTCACCACCTTCT

Fwd, Forward; Rev, Reverse.

Investigative Ophthalmology & Visual Science

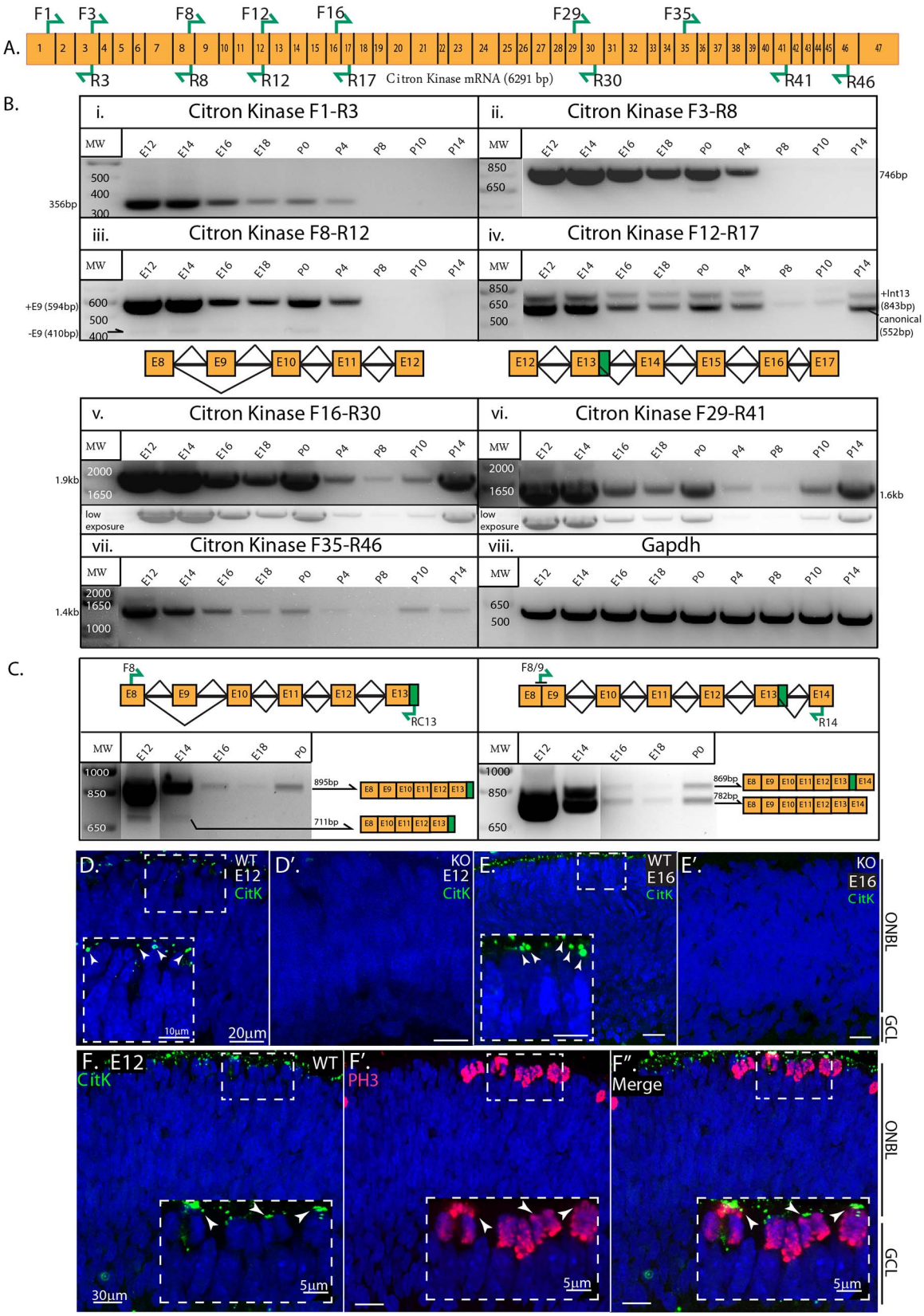

Figure 1. Expression analysis of citron kinase during rat retinal development. (**A**) Schematic representation of *CitK* mRNA showing exons (*orange boxes*) and the primers (*green arrows*) used for RT-PCR analysis. (**B**) Gel images showing the expression of *CitK* at retinal time points indicated on *top* along with the forward and reverse primers used. Primers in (**i**) exons 1 and 3; (**ii**) exons 3 and 8; (**iii**) exons 8 and 12; (**iv**) exons 12 and 17, with schematic representation of isoforms detected in (**iii**) and (**iv**); (**v**) exons 16 and 30; (**vi**) exons 29 and 41; (**vii**) exons 35 and 46; and (**viii**) *Gapdh*. (**vi**, **vii**) Gel images at the *bottom* show a low exposure image. (**C**) Schematic representation of combination of isoforms identified in *CitK* and the primers used for RT-PCR analysis (*green arrows*, F8–RC13 and F8/9–R14). *Left*: Gel image showing the expression of isoform containing

Investigative Ophthalmology & Visual Science

cryptic donor in exon 13 along with or without exon 9 included across E12, E14, E16, E18, and P0. *Right*: Gel image showing the expression of isoform containing exon 9 with or without cryptic donor in exon 13 across E12, E14, E16, E18, and P0. (**D–E'**) Immunohistochemistry with mouse-CitK antibody (*green*) on E12 WT (**D**) and KO (**D'**) retinae and E16 WT (**E**) and KO (**E'**) retinae. *Insets* show the localization of CitK (*arrowheads*). (**F–F"**) Immunohistochemistry with mouse anti-CitK antibody (*green*) along with rabbit anti-PH3 antibody (*red*) on E12 retinal sections. DAPI (*blue*) marks all the nuclei.

formed on E16 retinal sections. The sections were then fixed and TUNEL assay was carried out.

Image Acquisition and 3-D Reconstruction

Confocal fluorescence microscopy was performed with Leica SP2 (Leica Microsystems, Inc., Buffalo Grove, IL, USA). Images were subsequently processed by using IMARIS 7.3 (Bitplane, Inc., South Windsor, CT, USA) and Adobe Photoshop CS4 (Adobe Systems, Inc., San Jose, CA, USA). For counting, spot tool in IMARIS software was used. For confirming the overlap between Ki67 and TUNEL signal, section tool was used. The placement of the cross hairs shows the signal in the longitudinal (shown on right) and horizontal axis (shown at the bottom) at the given position.

Statistical Analysis

Data were analyzed in Microsoft Excel 2007 (Microsoft Corp., Redmond, WA, USA). Statistical significance was determined by using the Student's *t*-test ($P \leq 0.05$). Data are presented as mean ± SEM.

Results

Citron Kinase Is Enriched During Embryonic Retinal Development

CitK has 47 exons with exons 1 through 12 encoding the kinase domain. Upstream of exon 12, there is an alternative transcription start site that is used to produce a truncated protein called Citron N, lacking the kinase domain.[25] Polymerase chain reaction (PCR) amplification of the region coding for the kinase domain with primers F1–R3 and F3–R8 (shown as green arrows in Fig. 1A) showed a trend with robust expression starting at embryonic day (E)12 followed by a steady decline leading to absence by postnatal day (P)8 (Fig. 1B.i, ii). However, primer pairs (F12–R17) showed that the alternative transcription start site upstream of exon 12 was being used at P10 and P14 (Fig. 1B.iv). This was further confirmed by F16–R30 and F29–R41 primer pairs that showed a robust PCR product at P14 and lower levels at P8 and P10 (Fig. 1B.v, vi). Interestingly, this was not the case for F35–R46 primer pairs where the levels were not similar (Fig. 1B.vii). The identity of the upper band observed in E12 with F35–R46 primers was not interrogated (Fig. 1B.vii). Moreover, PCR with

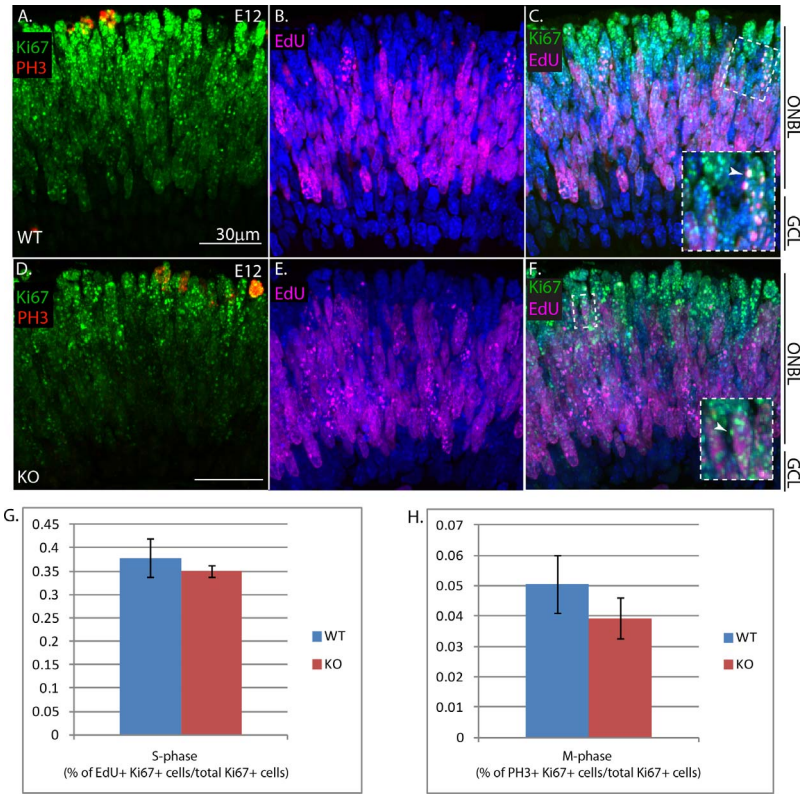

Figure 2. Number of progenitor cells in WT and KO retinae is comparable at E12. Immunohistochemistry on retinal sections obtained from embryonic day E12 embryos where the mother was pulsed with EdU 1 hour before harvest. (**A**, **D**) Retinal progenitor cells positive for Ki67 (*green*) and PH3 (*red*) in WT (**A**) and KO (**D**). (**B**, **E**) Retinal progenitor cells positive for EdU (*magenta*) in WT (**B**) and KO (**E**). DAPI (*blue*) marks all nuclei. (**C**, **F**) Merged image showing RPCs positive for Ki67 (*green*) and EdU (*magenta*) in WT (**C**) and KO (**F**). DAPI (*blue*) marks all nuclei. *Inset* shows the higher magnification image of the *boxed region* in the apical end of the ONBL where the *solid arrow* points to an RPC that is EdU+ and Ki67+. (**G**) Quantification of S-phase RPCs (EdU+ cells) as a percentage of all RPCs (Ki67+ cells) in WT (*blue*, $n = 6$) and KO (*red*, $n = 9$). (**H**) Quantification of M-phase RPCs (PH3+ cells) as a percentage of all RPCs (Ki67+ cells) in WT (*blue*, $n = 6$) and KO (*red*, $n = 9$).

Investigative Ophthalmology & Visual Science

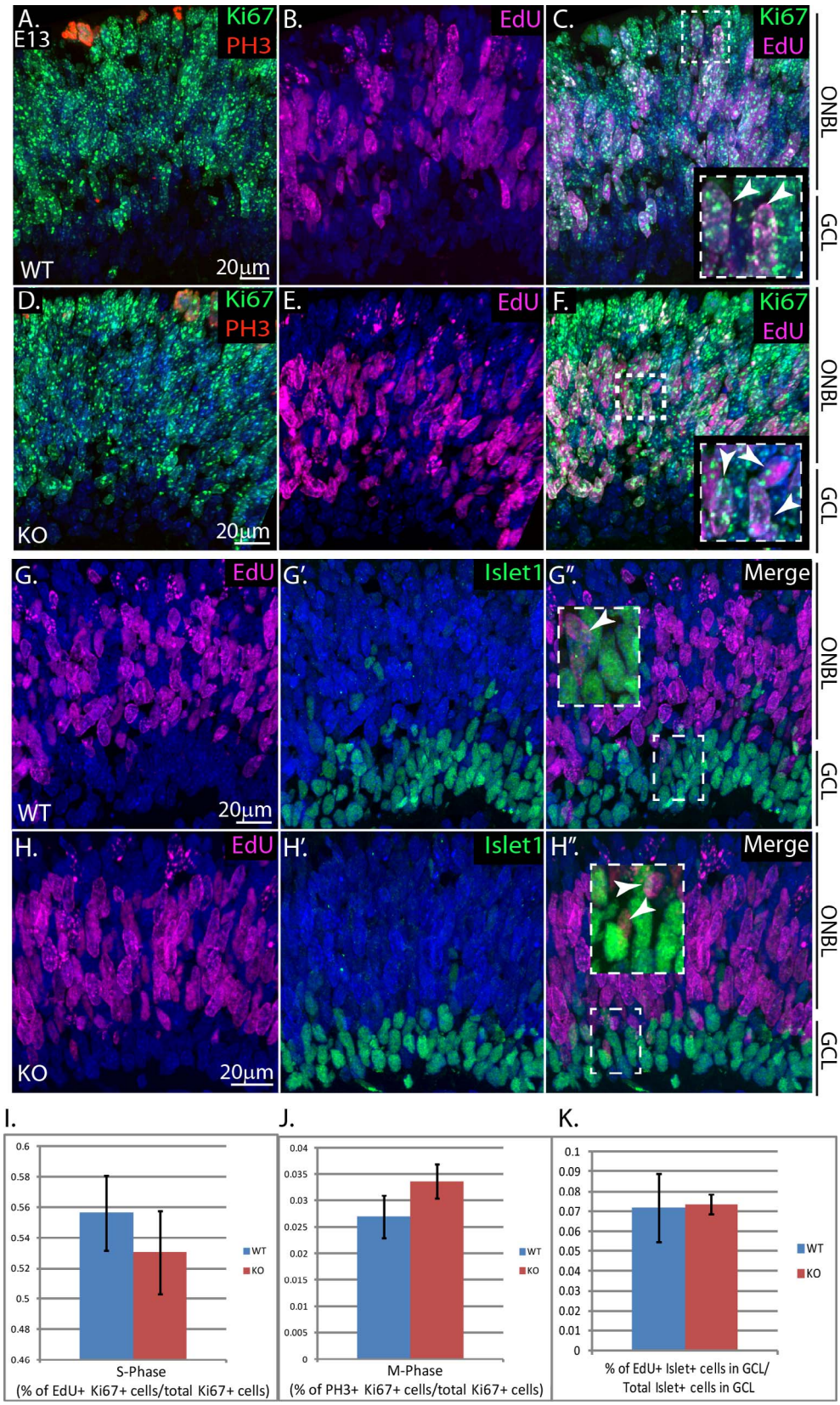

Figure 3. Number of RPCs and RGCs in WT and KO retinae is comparable at E13. Immunohistochemistry on retinal sections obtained from E13 embryos where the mother was pulsed with EdU at E12. (**A**, **D**) Retinal progenitor cells positive for Ki67 (*green*) and PH3 (*red*) in WT (**A**) and KO (**D**). (**B**, **E**) Retinal progenitor cells positive for EdU (*magenta*) in WT (**B**) and KO (**E**). (**C**, **F**) Merged image showing RPCs positive for Ki67 (*green*) and EdU (*magenta*) in WT (**C**) and KO (**F**). DAPI (*blue*) marks all nuclei. *Inset* shows the higher magnification image of the *boxed region* in the apical end of the ONBL where the *solid arrow* points to an RPC that is EdU+ and Ki67+. (**G–H"**) Retinal sections showing EdU+ cells (*magenta*) in WT (**G**) and KO (**H**) along with IHC for Islet1 (*green*) in WT (**G'**) and KO (**H'**). Shown in (**G"**) and (**H"**) are the merged images of (**G**) and (**G'**) and

Investigative Ophthalmology & Visual Science

(**H**) and (**H'**), respectively. *Inset* shows the higher magnification image of the *boxed region* in the GCL where the *solid arrow* points to an RGC that is EdU+ and Islet1+. DAPI (*blue*) marks all nuclei. (**I**) Quantification of S-phase RPCs (EdU+ cells) as a percentage of all RPCs (Ki67+ cells) in WT (*blue*, $n = 7$) and KO (*red*, $n = 10$). (**J**) Quantification of M-phase RPCs (PH3+ cells) as a percentage of all RPCs (Ki67+ cells) in WT (*blue*, $n = 7$) and KO (*red*, $n = 10$). (**K**) Quantification of RGCs born at/after E12 by determining Islet1+ and EdU+ cells as a percentage of all Islet1+ cells within the GCL in WT (*blue*, $n = 3$) and KO (*red*, $n = 7$).

the primer pair F8–R12 (positions shown in Fig. 1A) showed two bands at 594 bp and 410 bp (Fig. 1B.iii). Sequence analysis of both these isoforms revealed that the isoform at 594 bp was the canonical isoform including all exons in between. The lower molecular weight (MW) isoform at 410 bp lacked exon 9 (schematic representation below Fig. 1B.iii). For the primers (F12–R17) amplifying the region between exon 12 and exon 17, there were two bands at 843 bp and 552 bp (Fig. 1B.iv). Again, sequence analysis of both these isoforms revealed that the isoform at 552 bp was the canonical isoform including all exons, while the higher MW isoform at 843 bp was produced by (schematic representation below Fig. 1B.iv) the usage of the cryptic splice donor at 42306705 NT position (NCBI reference: AC_000080.1) (AGT/GTAG) in intron 13. Since our analysis interrogated short stretches of CitK mRNA, we could not determine the specific combinations in which the two alternative splicing events were used. For this, we designed a new set of primers (Fig. 1C, schematic representation) in cryptic donor region in exon 13 and junction of exon 8 and 9. The RT-PCR analysis with F8–RC13 showed that there were two bands obtained at E12 and E14. The higher MW band at 895 bp corresponds to the isoform containing a part of retained intron 13 along with exon 9 included, while the lower MW isoform at 711 bp excludes exon 9 (Fig. 1C, left). From E16 onward, only the higher MW isoform was observed. Analysis was not carried out beyond P0, as *CitK* expression shuts down postnatally. To find whether exon 9 is expressed with the isoform containing canonical exon 13, RT-PCR analysis with F8/9–R14 was performed. Analysis showed that there were two bands obtained across development with a robust expression observed at E12. The higher MW band at 869 bp corresponds to isoform containing exon 9 with a part of intron 13 retained, and the lower MW band at 782 bp corresponds to the isoform with exon 9 and canonical exon 13 (Fig. 1C, right).

Next, we interrogated the expression of CitK protein by section IHC in E12 and E16 retinae. This analysis showed CitK localized in discrete puncta at the apical tip, where RPCs undergo M-phase of the cell cycle (Figs. 1D, 1E, insets). This observation is in agreement with the report by Di Cunto et al.,[25] who have reported expression of CitK in the developing retina by whole-mount in situ hybridization at E11.5 when there are only RPCs, which suggests expression of CitK in RPCs. Moreover, in the developing brain, CitK expression is found at the cytokinesis furrow in progenitor cells.[22] Thus, expression of CitK was considered to be in RPCs. Absence of signal in the KO retina confirmed specificity of the CitK antibody (Figs. 1D', 1E'). Finally, to confirm whether the punctuate staining of CitK corresponds to RPCs, E12 sections were costained with anti-PH3 antibody (marks M-phase progenitor cells [Fig. 1F']), which showed overlap in signal for PH3 and CitK (Figs. 1F–F", inset).

Number of Progenitor Cells in the KO Retina Is Comparable to That in the WT Retina at E12 and E13

Given the robust expression of *CitK* in early RPCs, we wanted to interrogate its role in retinal development. For this, we pulsed pregnant female rats at E12 with EdU 1 hour before harvest. The E12 WT and KO retinal sections were then

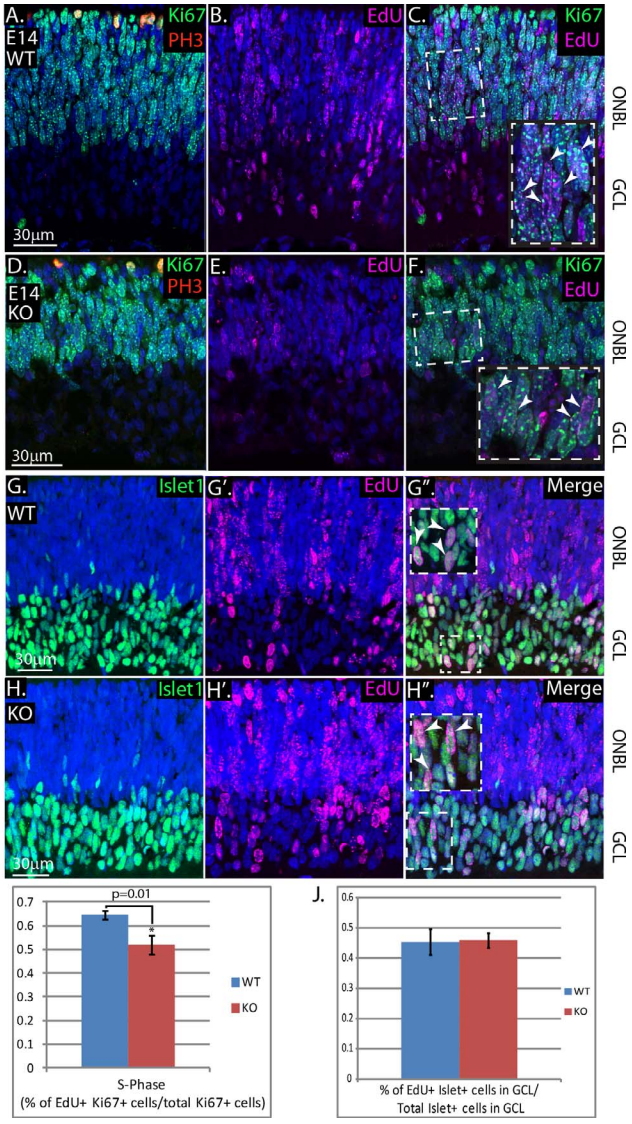

Figure 4. Number of RGCs in WT and KO retinae is comparable at E14 but the number of RPCs in S-phase are fewer in the KO retina. Immunohistochemistry on retinal sections obtained from E14 embryos where the mother was pulsed with EdU at E12. (**A**, **D**) Retinal progenitor cells positive for Ki67 (*green*) and PH3 (*red*) in WT (**A**) and KO (**D**). (**B**, **E**) Retinal progenitor cells positive for EdU (*magenta*) in WT (**B**) and KO (**E**). (**C**, **F**) Merged image showing RPCs positive for Ki67 (*green*) and EdU (*magenta*) in WT (**C**) and KO (**F**). DAPI (*blue*) marks all nuclei. *Inset* shows the higher magnification image of the *boxed region* in the apical end of the ONBL where the *solid arrow* points to an RPC that is EdU+ and Ki67+. (**G–H"**) Retinal sections showing EdU+ cells (*magenta*) in WT (**G**) and KO (**H**) along with IHC for Islet1 (*green*) in WT (**G'**) and KO (**H'**). Shown in (**G"**) and (**H"**) are the merged images of (**G**) and (**G'**) and (**H**) and (**H'**), respectively. *Inset* shows the higher magnification image of the *boxed region* in the GCL where the *solid arrow* points to an RGC that is EdU+ and Islet1+. DAPI (*blue*) marks all nuclei. (**I**) Quantification of S-phase RPCs (EdU+ cells) as a percentage of all RPCs (Ki67+ cells) in WT (*blue*, $n = 3$) and KO (*red*, $n = 9$); Student's *t*-test, $P = 0.01$. (**J**) Quantification of RGCs born after E12 by determining Islet1+ and EdU+ cells as a percentage of all Islet1+ cells within the GCL in WT (*blue*, $n = 6$) and KO (*red*, $n = 7$).

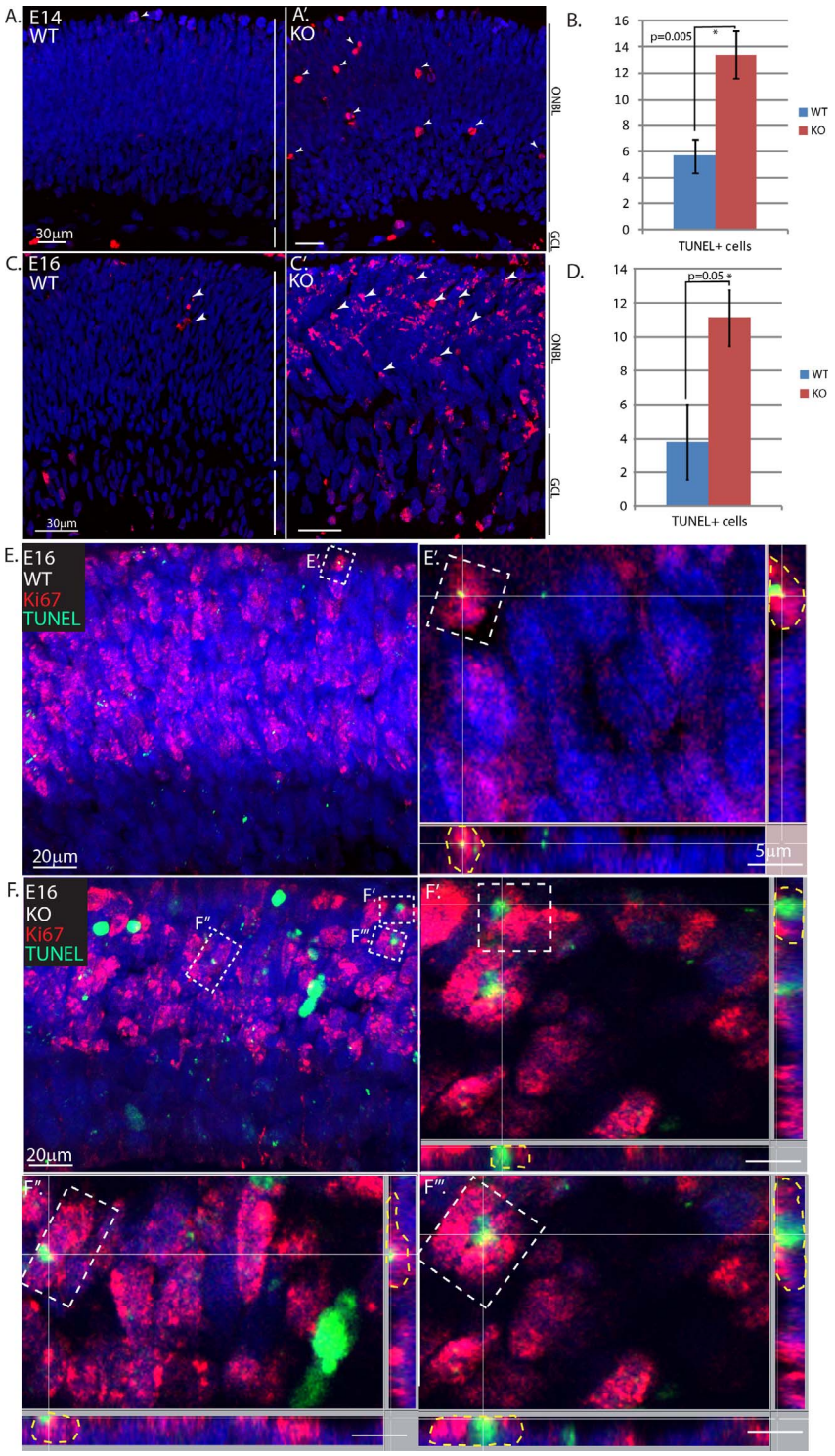

Figure 5. Reduction in RPCs without change in RGCs between WT and KO retinae at E16. (**A**, **A'**) TUNEL assay (*red*) on E14 WT (**A**) and KO (**A'**) retinae. DAPI (*blue*) marks all the nuclei. (**B**) Quantification showing cell death (TUNEL+ in [**A**] and [**A'**]) in E14 WT (*blue*, $n = 6$) and KO (*red*, $n = 8$) retinal sections; Student's *t*-test, $P = 0.005$. (**C**, **C'**) TUNEL assay (*red*) on E16 WT (**C**) and KO (**C'**) retinae. DAPI (*blue*) marks all the nuclei. (**D**) Quantification showing cell death (TUNEL+ in [**C**] and [**C'**]) in E16 WT (*blue*, $n = 3$) and KO (*red*, $n = 6$) retinal sections; Student's *t*-test, $P = 0.05$. (**E**–**F'''**) Identity of TUNEL+ cells by IHC for Ki67 (*red*) and TUNEL (*green*) in E16 WT (**E**) and KO (**F**) retinal sections. The *boxed region* in (**E**) is shown as a high magnification image in (**E'**) with section function in IMARIS showing the overlap of cells positive for both Ki67 and TUNEL (details in Materials and Methods). *Boxed regions* in (**F**) are shown as high magnification images in (**F'**–**F'''**) with section function in IMARIS showing the overlap of cells positive for both Ki67 and TUNEL.

Investigative Ophthalmology & Visual Science

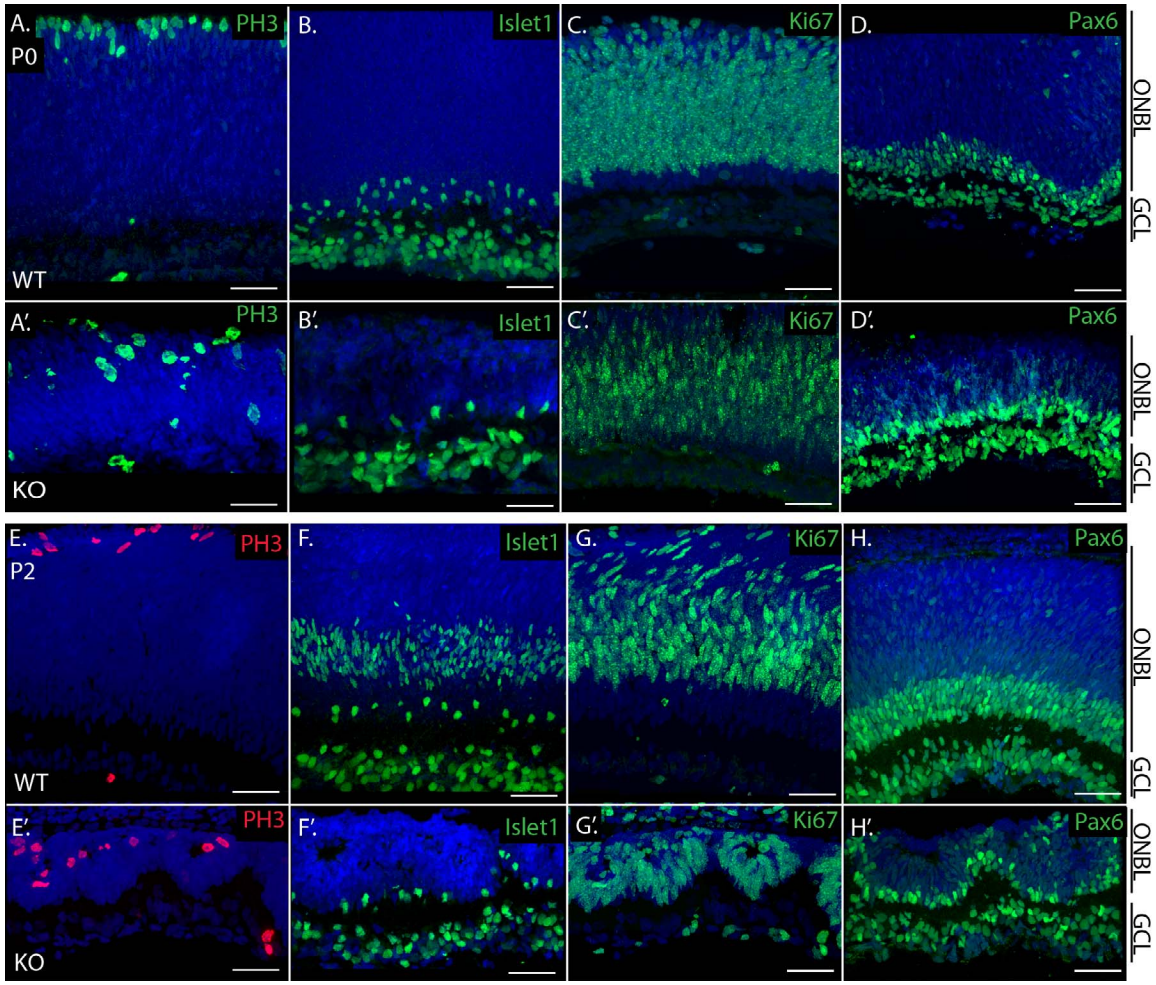

Figure 6. Reduction in the ONBL in the CitK KO retina along with absence of bipolar cells at P2. (**A–D'**) Immunohistochemistry on P0 retinal section showing PH3 (*green*) in WT (**A**) and KO (**A'**); Islet1 (*green*) in WT (**B**) and KO (**B'**); Ki67 (*green*) in WT (**C**) and KO (**C'**); and Pax6 (*green*) in WT (**D**) and KO (**D'**). (**E–H'**) Immunohistochemistry on P2 retinal section showing PH3 (*red*) in WT (**E**) and KO (**E'**); Islet1 (*green*) in WT (**F**) and KO (**F'**); Ki67 (*green*) in WT (**G**) and KO (**G'**); and Pax6 (*green*) in WT (**H**) and KO (**H'**). DAPI (*blue*) marks all the nuclei.

subjected to IHC with anti-Ki67, PH3, along with EdU detection (Figs. 2A–F). Here, we quantified EdU+ (in S-phase) RPCs as a percentage of total Ki67+ RPCs, which showed no difference in S-phase RPCs in *CitK* KO compared to WT (Fig. 2G). Similarly, PH3+ (M-phase) RPCs as a percentage of total Ki67+ RPCs did not show any difference between KO and WT (Fig. 2H).

Next, we wanted to interrogate the effect of loss of CitK on RPCs over time. So, we performed an EdU pulse-chase experiment. For this, we pulsed pregnant females at E12 followed by harvest at E13. Again, WT and KO retinal sections were subjected to Ki67, PH3, along with EdU detection (Figs. 3A–F). The EdU+ RPCs (S-phase) as a percentage of total Ki67+ RPCs did not change in KO compared to WT (Fig. 3I). This was also true for PH3+ (M-phase) RPCs (Fig. 3J). Since RPCs did not show an observable phenotype in *CitK* KO retina, we wanted to interrogate if neurogenesis was affected. Since retinal ganglion cells (RGCs) were the only cell type produced at this point, we used Islet1 antibody to mark the RGCs. Specifically, we looked for Islet1+ cells that were also EdU+, so as to interrogate RGCs produced after the EdU pulse (Figs. 3G–H"). Again, we did not see a significant difference in RGC production in KO compared to WT (Fig. 3K).

Cell Death of a Subset of Progenitor Cell Population Is Observed in the KO Retina by E14

Next, we pulsed E12 pregnant females with EdU followed by embryo harvest at E14. Retinal sections from KO and WT embryos were subjected to IHC with Ki67, PH3, along with EdU detection (Figs. 4A–F). Quantification of EdU+ (S-phase) RPCs as a percentage of total Ki67+ RPCs showed statistically significant decrease in RPCs in the *CitK* KO compared to WT (Fig. 4I). This suggested that there was a loss of RPCs in the *CitK* KO retina, which suggests that either the RPCs died or there was an increase in RGC production at the expense of these RPCs. To distinguish between these two possibilities, we performed IHC with Islet1 along with EdU detection (Figs. 4G–H"). Quantification was restricted to the ganglion cell layer (GCL) to take into account only the differentiated ganglion cells and not include newly born Islet1+ RGCs or amacrine cells (ACs) in the ONBL. Quantification of Islet1+ cells that were also EdU+ as a percentage of total Islet1+ cells in the GCL did not show a statistically significant difference in KO compared to WT (Fig. 4J). This led us to interrogate the possibility that RPCs were undergoing cell death in *CitK* KO retinae. Indeed, TUNEL analysis showed increased cell death in *CitK* KO compared to WT (Figs. 5A, 5A', 5B).

Investigative Ophthalmology & Visual Science

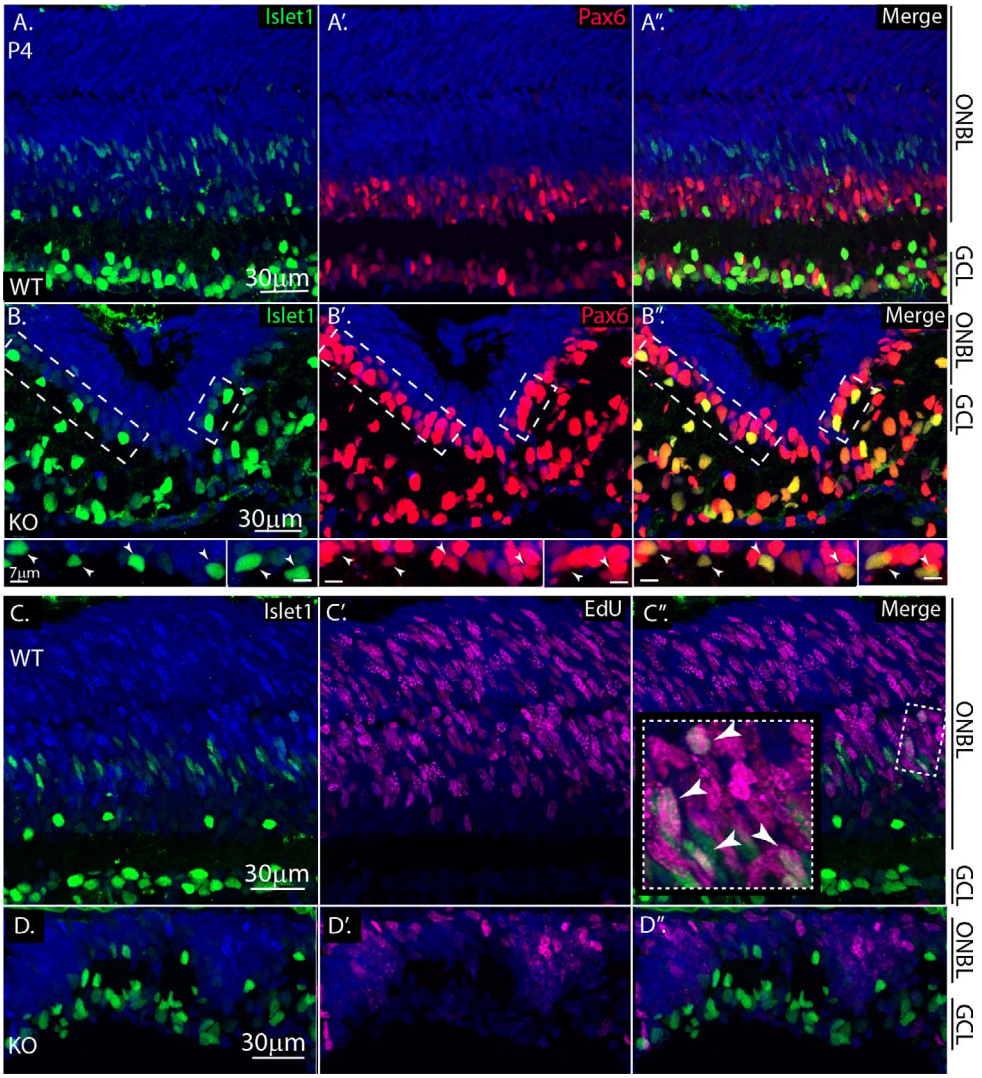

Figure 7. Bipolar cells are not produced in the KO retina at P4. (**A–B"**) Immunohistochemistry on P4 retinal sections for Islet1 (*green*) in WT (**A**) and KO (**B**) and for Pax6 (*red*) in WT (**A'**) and KO (**B'**). Merged images of (**A**) and (**A'**) and (**B**) and (**B'**) are shown in (**A"**) and (**B"**), respectively. Higher magnification images of dashed box in (**B–B"**) highlight the cells (marked by *arrowheads*) that are both Islet1+ and Pax6+. (**C–D"**) Immunohistochemistry on sections of P4 retinae harvested from rats pulsed with EdU at P0. Expression of Islet1 (*green*) in WT (**C**) and KO (**D**) and EdU detection in WT (**C'**) and KO (**D'**). Merged images of (**C**) and (**C'**) and (**D**) and (**D'**) are shown in (**C"**) and (**D"**), respectively. *Inset* in (**C"**) shows a higher magnification image of the *boxed region* highlighting bipolar cells born at/after P0. DAPI marks all the nuclei.

Similar analysis was extended to E16 retinae that were harvested from embryos where the mother had been pulsed with EdU at E12. Here, a significant decrease in the size of the ONBL and a concomitant increase in TUNEL+ cells in KO retina were observed (Figs. 5C, 5C', 5D). To confirm that the TUNEL+ cells were RPCs, sections that were subjected to TUNEL assay were stained for Ki67. Here, we observed that many TUNEL+ cells were Ki67+ as well (Figs. 5E–F"'). The overlap was confirmed by using section tool in IMARIS 7.3 software, where the cross hairs mark the cell under interrogation, with the panel on the right showing the longitudinal axis and the one at the bottom showing the horizontal axis. In both cases, overlap was observed for TUNEL and Ki67 positivity (Figs. 5E', 5F'–F"'). However, there were some cells that were TUNEL+ but Ki67– in the ONBL. These cells had increased intensity of TUNEL signal, which correlates with the extent of cell death; moreover, lack of Ki67 positivity might be due to protein degradation.

Absence of Islet1+ Bipolar Cell Production in the KO Retina

The increase in cell death of RPCs after E14 led us to extend our analysis to the postnatal development. At P0, the KO retinal tissue was visibly smaller than the WT retina. Immunohistochemistry analysis with different markers, such as anti-PH3, anti-Islet1, anti-Ki67, and anti-Pax6 antibodies, showed that GCL remained uncompromised (Figs. 6A–D'). However, the ONBL was half the size of the WT counterpart and showed signs of rosette formation. However, PH3 and Ki67+ RPCs were observed in the P0 CitK KO retina (Figs. 6A', 6C'). Similarly, Islet1+ and Pax6+ RGCs and ACs were observed in the KO retina (Figs. 6B', 6D'). Interestingly, at P2, Islet1+ RGCs and ACs were observed in the WT and KO retinae (Figs. 6F, 6F'). However, Islet1+ bipolar cells (BPCs)[27] were not observed in the KO retinae (Fig. 6F'). Similarly, Pax6+ RGCs and ACs were observed in the WT and KO retinae (Fig. 6H, 6H'). Overall, the KO retinae showed rosette formation but

Investigative Ophthalmology & Visual Science

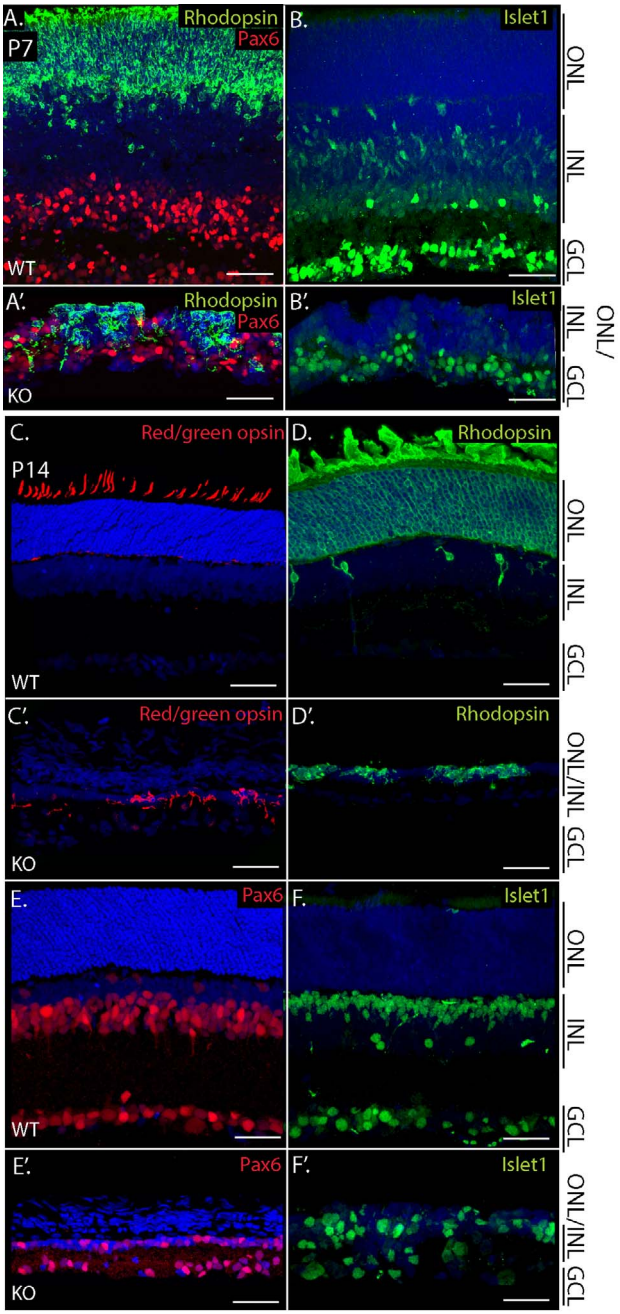

Figure 8. The KO retina is severely compromised by P14. (**A–B'**) Immunohistochemistry on P7 retinal sections showing rhodopsin (*green*) and Pax6 (*red*) in WT (**A**) and KO (**A'**); and Islet1 (*green*) in WT (**B**) and KO (**B'**). (**C–F'**) Immunohistochemistry on P14 retinal sections showing red/green opsin (*red*) in WT (**C**) and KO (**C'**); rhodopsin (*green*) in WT (**D**) and KO (**D'**); Pax6 (*red*) in WT (**E**) and KO (**E'**); and Islet1 (*green*) in WT (**F**) and KO (**F'**). DAPI marks all the nuclei.

some PH3+ and Ki67+ RPCs were still observed (Figs. 6E', 6G') like in their WT counterparts (Figs. 6E, 6G). At P4, the KO retina was structurally compromised with large rosettes in the ONBL. Again, Islet1 marked a subset of BPCs in the WT retina but these cells were not observed in the KO retina (Figs. 7A, 7B). To distinguish between BPCs and ACs in the ONBL, Pax6 was used to mark amacrine cells (Figs. 7A', 7A", 7B', 7B"). Thus, cells positive for both Islet1 and Pax6 revealed ACs in the ONBL, while those positive for Islet1 alone marked BPCs (Figs. 7A–A"; 7B–B", boxed region). To interrogate whether KO

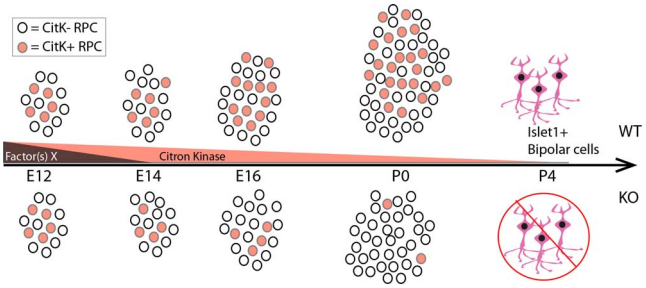

Figure 9. Model of the effect of loss of citron kinase on RPCs. Shown here is a developmental time line starting with E12 and P4. *Top panel* reflects the scenario in WT retinae and the *bottom panel* reflects the scenario in KO retinae. The *orange triangle* shows the expression levels of CitK as it decreases over time. The *brown triangle* shows the expression kinetics of a potential compensatory factor (factor X), which decreases by E14. The *circles* represent RPCs, where *open circles* represent CitK-ve RPCs, while *solid circles* (*orange*) represent CitK+ RPCs. The loss of CitK does not affect RPCs at E12 but is required for the survival of RPCs beginning at E14, shown as reduction in the number of *solid circles* in the KO scenario. This reduction in CitK+ RPCs results in drastic loss by P0 such that Islet1+ bipolar cells are not produced in the KO retinae.

retina failed to produce BPCs, we pulsed P0 pups with EdU, followed by retinal harvest at P4 and IHC with Islet1 and EdU (Figs. 7C–D"). This analysis showed that Islet1+ EdU+ BPCs were indeed produced in the WT retina (Fig. 7C", inset) but were not observed in the KO retina. However, EdU+ cells were observed in the ONBL of the KO retina (Fig. 7D").

CitK KO Retina Undergoes Severe Degeneration by P14

Immunohistochemistry analysis at P7 with rhodopsin showed that the properly laminated WT retina (Fig. 8A) and the KO retina had rhodopsin+ cells but the latter lacked lamination or canonical morphologic characteristics (Fig. 8A'). Similar to P4, Islet1 staining at P7 showed Islet1+ BPCs, RGCs and ACs in the WT retina (Fig. 8B) but the KO lacked the Islet1+ BPCs (Fig. 8B'). At P14, the KO retina had deteriorated such that the outer nuclear layer (ONL) and inner nuclear layer (INL) collapsed to a thin layer of cells that showed positivity for markers such as red/green opsin and rhodopsin (Figs. 8C–D'). However, the RGC layer was still present and positive for Islet1 and Pax6 (Figs. 8E–F').

Discussion

Role of Alternative Splicing in Citron Kinase Expression

Here we discovered an alternatively spliced isoform of *CitK* that is developmentally regulated such that exon 9 is excluded at E12 and E14. The amino acids encoded by exon 9 are 370–431 amino acids and are part of the kinase domain. Thus, the isoform lacking exon 9 would most likely lack the kinase function. In addition, we discovered another alternatively spliced isoform where there is cryptic donor in intron 13 such that it adds 29 amino acids. These amino acids are added to the structural maintenance of chromosome (SMC) domain, which could alter the nuclear function of *CitK*; this has been reported in drosophila where its homolog (called sticky) is required for heterochromatin-mediated gene silencing through HP1 localization and H3-K9 methylation.[28]

Retinal Progenitor Cell Death Does Not Begin Until E14

At E12, RT-PCR analysis showed highest levels of expression of *CitK*, but its loss did not affect RPCs at E12 or E13. This suggests that RPCs at E12 and E13 retina may have a compensatory mechanism that allows RPCs to undergo cytokinesis in the absence of *CitK*. By E14, we begin to see reduction in RPCs, which is coincident with TUNEL+ cells, suggesting *CitK* requirement for RPCs. Interestingly, RGC production was not aberrant in *CitK* KO retinae, which is in agreement with the observation that RPCs at E12 and E13 remain uncompromised. Indeed, it is at E12 that RGC production begins and resistance of E12 RPCs to loss of *CitK* allows for normal RGC production. The observation of cell death beginning at E14 raises the issue as to why it happens at E14 and not earlier (Fig. 9). One possibility is that a compensatory gene or genes (factor[s] X) exist(s) that allowed RPCs to survive at E12 and E13 and this gene (or these genes) was (were) downregulated by E14 (Fig. 9). Other Rho-dependent kinases, such as Rho-associated protein kinase (*ROCK*) and *Cdc42*, have been shown to play a regulatory role in the contractility of the cleavage furrow during cytokinesis.[12,13,29,30] *Aurora*, another member of serine/threonine kinase family, and Aurora and Ipl1-like midbody-associated protein (*AIM-1*) have also been shown to play a critical role in cell division especially at the midbody furrow.[31,32] *Nir1*, a mammalian homolog of retinal degeneration B in drosophila, has been shown to have a very similar function to that of *CitK*.[33] Therefore, it is possible that one or all of these genes could compensate for loss of *CitK* function.

Late Embryonic and Postnatal Neurogenesis Is Affected in the KO Retina

The depletion of RPCs that began at E14 reached its peak at E16, resulting in a severely compromised retina at birth. Notably, pulse-chase experiments with EdU showed that RPCs that were in S-phase at E12 (time of EdU pulse) had survived cell cycle and had re-entered cell cycle at E16, as shown by EdU+ cells that were Ki67+ (data not shown). These cells survived because they most likely did not express *CitK* or if they did express *CitK*, they also had the aforementioned compensatory factor(s). This agrees with the observation that only ~50% of neurogenic cytokineses in the brain are affected.[24] Thus, it is possible that RPCs can be grouped into two categories of neurogenic cytokinesis: one that is dependent on *CitK* and susceptible to cell death in the KO retina and the other that is independent of *CitK*, which results in RPCs that remain at P0 (Fig. 9). Moreover, the RPCs in the P0 KO retina fail to produce BPCs, as shown by the pulse-chase experiments where RPCs that took up EdU at P0 (time of pulse) did not show EdU+ Islet1+ BPCs at P4. It is also possible that RPCs in the KO retina failed to undergo cell division as a secondary effect of the severely compromised retina. This possibility is unlikely because there are distinct EdU+ nuclei in the ONBL of P4 retina, which suggests that the progeny of the progenitor cells that took up EdU were still alive (Fig. 7B1"). In all, our data showed that loss of *CitK* did not affect early embryonic RPCs, resulting in normal neurogenesis while altering late embryonic RPCs affecting subsequent neurogenesis.

Here we present a model in which a subset of RPCs required *CitK* function and this subset of progenitor cells went on to produce Islet1+ BPCs (Fig. 9, top). In the absence of *CitK*, expression of factor(s) X allows RPCs to survive until E14, when the levels of this (or these) factor(s) drop, making *CitK* function crucial for RPC survival. This in turn results in the death of these RPCs such that none are left at birth to produce the Islet1+ BPCs in the *CitK* KO retina (Fig. 9, bottom).

Acknowledgments

We thank Joseph Loturco (Physiology and Neurobiology Department, University of Connecticut, Storrs) for generously sharing the *CitK*-KO rats. We also thank Komal Patel and Matthew Girgenti from the laboratory of Joseph Loturco for helping us troubleshoot the genotyping protocol and the assessment of embryonic time points in the pregnant females.

Supported by grants from National Eye Institute (4R00EY019547) and National Institutes of Neurological Disorders and Stroke (5P30NS069266) (to RK).

Disclosure: **D.K.P. Karunakaran**, None; **N. Chhaya**, None; **C. Lemoine**, None; **S. Congdon**, None; **A. Black**, None; **R. Kanadia**, None

References

1. Wong LL, Rapaport DH. Defining retinal progenitor cell competence in Xenopus laevis by clonal analysis. *Development*. 2009;136:1707–1715.
2. He J, Zhang G, Almeida AD, Cayouette M, Simons BD, Harris WA. How variable clones build an invariant retina. *Neuron*. 2012;75:786–798.
3. Cepko CL, Austin CP, Yang X, Alexiades M, Ezzeddine D. Cell fate determination in the vertebrate retina. *Proc Natl Acad Sci U S A*. 1996;93:589–595.
4. Livesey FJ, Cepko CL. Vertebrate neural cell-fate determination: lessons from the retina. *Nat Rev Neurosci*. 2001;2:109–118.
5. Turner DL, Cepko CL. A common progenitor for neurons and glia persists in rat retina late in development. *Nature*. 1987;328:131–136.
6. Jensen AM, Raff MC. Continuous observation of multipotential retinal progenitor cells in clonal density culture. *Dev Biol*. 1997;188:267–279.
7. Marquardt T, Ashery-Padan R, Andrejewski N, Scardigli R, Guillemot F, Gruss P. Pax6 is required for the multipotent state of retinal progenitor cells. *Cell*. 2001;105:43–55.
8. Hafler BP, Surzenko N, Beier KT, et al. Transcription factor Olig2 defines subpopulations of retinal progenitor cells biased toward specific cell fates. *Proc Natl Acad Sci U S A*. 2012;109:7882–7887.
9. Buchman JJ, Tsai LH. Putting a notch in our understanding of nuclear migration. *Cell*. 2008;134:912–914.
10. Del Bene F. Interkinetic nuclear migration: cell cycle on the move. *EMBO J*. 2011;30:1676–1677.
11. Silva AO, Ercole CE, McLoon SC. Plane of cell cleavage and numb distribution during cell division relative to cell differentiation in the developing retina. *J Neurosci*. 2002;22:7518–7525.
12. Di Cunto F, Calautti E, Hsiao J, et al. Citron rho-interacting kinase, a novel tissue-specific ser/thr kinase encompassing the Rho-Rac-binding protein Citron. *J Biol Chem*. 1998;273:29706–29711.
13. Madaule P, Eda M, Watanabe N, et al. Role of citron kinase as a target of the small GTPase Rho in cytokinesis. *Nature*. 1998;394:491–494.
14. Eda M, Yonemura S, Kato T, et al. Rho-dependent transfer of Citron-kinase to the cleavage furrow of dividing cells. *J Cell Sci*. 2001;114:3273–3284.
15. Yamashiro S, Totsukawa G, Yamakita Y, et al. Citron kinase, a Rho-dependent kinase, induces di-phosphorylation of regulatory light chain of myosin II. *Mol Biol Cell*. 2003;14:1745–1756.

16. Matsumura F, Totsukawa G, Yamakita Y, Yamashiro S. Role of myosin light chain phosphorylation in the regulation of cytokinesis. *Cell Struct Funct*. 2001;26:639–644.
17. Gai M, Camera P, Dema A, et al. Citron kinase controls abscission through RhoA and anillin. *Mol Biol Cell*. 2011;22: 3768–3778.
18. Fu Y, Huang J, Wang KS, Zhang X, Han ZG. RNA interference targeting CITRON can significantly inhibit the proliferation of hepatocellular carcinoma cells. *Mol Biol Rep*. 2011;38:693–702.
19. Kamijo K, Ohara N, Abe M, et al. Dissecting the role of Rho-mediated signaling in contractile ring formation. *Mol Biol Cell*. 2006;17:43–55.
20. Gruneberg U, Neef R, Li X, et al. KIF14 and citron kinase act together to promote efficient cytokinesis. *J Cell Biol*. 2006; 172:363–372.
21. Neumann B, Walter T, Heriche JK, et al. Phenotypic profiling of the human genome by time-lapse microscopy reveals cell division genes. *Nature*. 2010;464:721–727.
22. Sarkisian MR, Li W, Di Cunto F, D'Mello SR, LoTurco JJ. Citron-kinase, a protein essential to cytokinesis in neuronal progenitors, is deleted in the flathead mutant rat. *J Neurosci*. 2002;22:RC217.
23. Cogswell CA, Sarkisian MR, Leung V, Patel R, D'Mello SR, LoTurco JJ. A gene essential to brain growth and development maps to the distal arm of rat chromosome 12. *Neurosci Lett*. 1998;251:5–8.
24. LoTurco JJ, Sarkisian MR, Cosker L, Bai J. Citron kinase is a regulator of mitosis and neurogenic cytokinesis in the neocortical ventricular zone. *Cereb Cortex*. 2003;13:588–591.
25. Di Cunto F, Imarisio S, Hirsch E, et al. Defective neurogenesis in citron kinase knockout mice by altered cytokinesis and massive apoptosis. *Neuron*. 2000;28:115–127.
26. Kanadia RN, Shin J, Yuan Y, et al. Reversal of RNA missplicing and myotonia after muscleblind overexpression in a mouse poly(CUG) model for myotonic dystrophy. *Proc Natl Acad Sci U S A*. 2006;103:11748–11753.
27. Elshatory Y, Deng M, Xie X, Gan L. Expression of the LIM-homeodomain protein Isl1 in the developing and mature mouse retina. *J Comp Neurol*. 2007;503:182–197.
28. Sweeney SJ, Campbell P, Bosco G. Drosophila sticky/citron kinase is a regulator of cell-cycle progression, genetically interacts with Argonaute 1 and modulates epigenetic gene silencing. *Genetics*. 2008;178:1311–1325.
29. Madaule P, Furuyashiki T, Eda M, Bito H, Ishizaki T, Narumiya S. Citron, a Rho target that affects contractility during cytokinesis. *Microsc Res Techniq*. 2000;49:123–126.
30. Amano M, Nakayama M, Kaibuchi K. Rho-kinase/ROCK: a key regulator of the cytoskeleton and cell polarity. *Cytoskeleton (Hoboken)*. 2010;67:545–554.
31. Glover DM, Leibowitz MH, McLean DA, Parry H. Mutations in aurora prevent centrosome separation leading to the formation of monopolar spindles. *Cell*. 1995;81:95–105.
32. Terada Y, Tatsuka M, Suzuki F, Yasuda Y, Fujita S, Otsu M. AIM-1: a mammalian midbody-associated protein required for cytokinesis. *EMBO J*. 1998;17:667–676.
33. Litvak V, Tian D, Carmon S, Lev S. Nir2, a human homolog of Drosophila melanogaster retinal degeneration B protein, is essential for cytokinesis. *Mol Cell Biol*. 2002;22:5064–5075.

Investigative Ophthalmology & Visual Science